

The pulsating sdB+M eclipsing system NY Virginis and its circumbinary planets

Jae Woo Lee,^{1,2*} Tobias Cornelius Hinse,^{1,3} Jae-Hyuck Youn¹ and Wonyong Han^{1,2}

¹Korea Astronomy and Space Science Institute, 776 Daedeokdae-ro, Yuseong-gu, Daejon 305-348, Korea

²Astronomy and Space Science Major, Korea University of Science and Technology, Daejeon 305-350, Korea

³Armagh Observatory, College Hill, BT61 9DG Armagh, UK

Accepted 2014 September 16. Received 2014 September 12; in original form 2014 June 24

ABSTRACT

We searched for circumbinary planets orbiting NY Vir in historical eclipse times including our long-term CCD data. 68 times of minimum light with accuracies better than 10 s were used for the ephemeris computations. The best fit to those timings indicated that the orbital period of NY Vir has varied due to a combination of two sinusoids with periods of $P_3 = 8.2$ yr and $P_4 = 27.0$ yr and semi-amplitudes of $K_3 = 6.9$ s and $K_4 = 27.3$ s, respectively. The periodic variations most likely arise from a pair of light-time effects due to the presence of third and fourth bodies that are gravitationally bound to the eclipsing pair. We have derived the orbital parameters and the minimum masses, $M_3 \sin i_3 = 2.8 M_{\text{Jup}}$ and $M_4 \sin i_4 = 4.5 M_{\text{Jup}}$, of both objects. A dynamical analysis suggests that the outer companion is less likely to orbit the binary on a circular orbit. Instead, we show that future timing data might push its eccentricity to moderate values for which the system exhibits long-term stability. The results demonstrate that NY Vir is probably a star-planet system, which consists of a very close binary star and two giant planets. The period ratio P_3/P_4 suggests that a long-term gravitational interaction between them would result in capture into a nearly 3:10 mean motion resonance. When the presence of the circumbinary planets is verified and understood more comprehensively, the formation and evolution of this planetary system should be advanced greatly.

Key words: binaries: close – binaries: eclipsing – stars: individual: NY Virginis – planetary systems.

1 INTRODUCTION

The presence of a third body causes the relative distance of the eclipsing pair to the observer to change as it orbits the barycentre of the triple system. The light-travel-time (LTT) effect produces a periodic variation in times of conjunction, which can be studied by searching for quasi-sinusoidal features in O–C diagrams (observed minus calculated minimum epochs). Eclipse times have been exploited since the late 18th century and their accuracies have increased significantly with the use of modern observations with high quantum efficiency. The timing method offers us an opportunity to detect circumbinary substellar companions, such as giant planets and brown dwarfs (BDs), for eclipsing binaries with timing accuracies of a few seconds, if their historical data base is large and sufficiently long (Lee et al. 2009a; Pribulla et al. 2012). Also, it should be possible to find additional planets or exomoons by analysing transit timing variations in systems with known transiting

planets (Doyle & Deeg 2004; Holman 2005). The discovery and interpretation of such objects is of great interest because they can help in understanding the diverse architectures of planetary systems.

In order to search for low-mass objects orbiting a close binary using timing measurements, we have been observing eclipsing stars, primarily HW Vir-type detached systems which consist of a subdwarf B (sdB) primary and a normal main-sequence (MS) M companion with orbital periods between 2 and 4 h. In our first result, we discovered two substellar companions revolving around the prototype HW Vir with orbital periods of 15.8 and 9.1 yr and having minimum masses of 19.2 and $8.5 M_{\text{Jup}}$, respectively, based on our photometric observations from 2000 to 2008 (Lee et al. 2009a). The circumbinary objects are the first planetary system unequivocally discovered using eclipse timings.

NY Vir (PG 1336-018, GSC 4966-491, 2MASS J13384814-0201491; $V = 13.3$) has been included as an object in our survey. The variable was recognized to be an HW Vir-like eclipsing binary of about 2.4 h period with a rapid sdB pulsator by Kilkenny et al. (1998). They determined the effective temperatures of $T_1 = 33\,000$ K and $T_2 = 3000$ K, the gravity of $\log g_1 = 5.7$,

* E-mail: jwlee@kasi.re.kr

Table 1. Observing log of NY Vir.

| Season | Observing interval | N_{night} | CCD type | FOV (arcmin 2) | N_{obs} |
|--------|------------------------|--------------------|-----------------|--------------------|------------------|
| 2011 | January 28–February 11 | 7 | FLI IMG4301E 2K | 22 × 22 | 468 |
| 2012 | February 01–02 | 2 | ARC 4K | 28 × 28 | 200 |
| 2013 | February 23–June 15 | 6 | ARC 4K | 28 × 28 | 1,133 |
| 2014 | March 08–May 24 | 2 | ARC 4K | 28 × 28 | 569 |

an orbital inclination of $i = 81^\circ$, and the relative radii of $r_1 = 0.19$ and $r_2 = 0.205$. Since then, the system has been the target of a Whole Earth Telescope campaign (Kilkenny et al. 2003) and the subject of several investigations (Kilkenny et al. 2000; Hu et al. 2007; Vučković et al. 2007, 2009), which have been reviewed in a recent paper by Kilkenny (2011). It is known that the primary component is a rapidly pulsating sdB star exhibiting short-period multimode light variations and the secondary is a fully convective M dwarf. In this paper, we present long-term CCD photometry of NY Vir and describe a search for circumbinary planets in this system from all available data. We then test the dynamical stability for our two-planet model and find several regions resulting in a stable orbital configuration over 10^6 yr.

2 NEW LONG-TERM OBSERVATIONS AND ECLIPSE TIMES

New CCD photometric observations of NY Vir were taken on 17 nights from 2011 January to 2014 May in order to collect additional eclipse timings. We used CCD cameras and I filters attached to the 1.0-m reflector at Mt Lemmon Optical Astronomy Observatory (LOAO) in Arizona, USA. A summary of the observations is listed in Table 1, where we present observing interval, numbers of nights, CCD type, field of view (FOV), and numbers of observed points. The instruments and reduction methods for the FLI IMG4301E and ARC 4K CCD cameras are the same as those described by Lee et al. (2009b, 2012b). In order to make an optimal artificial comparison source during our observing runs, we monitored a few tens of stars imaged on the chip at the same time as the eclipsing pair. Following the procedure described by Lee et al. (2011), five useful field stars were selected and combined by a weighted average. The difference magnitudes between the variable and the artificial reference star were computed and the resultant light curves are displayed in Fig. 1.

Over all observing seasons, 2370 individual observations were obtained and a sample of them is listed in Table 2, where times are Barycentric Julian Dates (BJD) in the Barycentric Dynamical Time system (Eastman, Siverd & Gaudi 2010). From the LOAO observations, times of minimum light and their errors were determined using the method of Kwee & van Woerden (1956). 43 new timings are given in Table 3; four of them are the weighted means calculated by us from the individual measurements of Vučković et al. (2007) in the $r'g'$ bandpasses of the SDSS system.

3 ECLIPSE TIMING VARIATION AND ITS IMPLICATIONS

Period studies of NY Vir have already been presented several times and the possible causes of the period variability have been discussed. From a quadratic fit, Kilkenny (2011) and Çamurdan, Çamurdan & İbanoğlu (2012) showed that the period is decreasing at a rate of -4.1×10^{-9} d yr $^{-1}$. The latter authors reported that the period decrease may be explained by an angular momentum loss (AML) from this system or may be only a part of a cyclic variation. Most

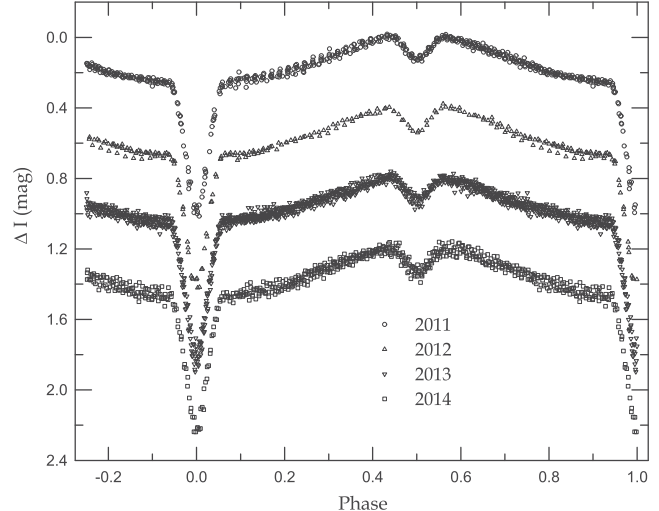


Figure 1. Light curves of NY Vir obtained at LOAO. The 2012–2014 curves are displaced vertically for clarity.

Table 2. I -band photometry of NY Vir. A sample is shown here; the full version is provided as supplementary material to the online article.

| BJD | Diff. mag | σ_{Mag} |
|----------------|-----------|-----------------------|
| 2455589.880291 | -0.0050 | 0.0070 |
| 2455589.881251 | 0.0073 | 0.0072 |
| 2455589.882212 | 0.0434 | 0.0073 |
| 2455589.883289 | 0.0721 | 0.0064 |
| 2455589.884481 | 0.1149 | 0.0064 |
| 2455589.885673 | 0.1218 | 0.0066 |
| 2455589.886865 | 0.1191 | 0.0064 |
| 2455589.888069 | 0.0966 | 0.0064 |
| 2455589.889261 | 0.0587 | 0.0060 |
| 2455589.890454 | 0.0175 | 0.0064 |

recently, from the analysis of 48 eclipse timings, Qian et al. (2012) found that the orbital period has varied through a combination of a downward parabola ($dP/dt = -3.36 \times 10^{-9}$ d yr $^{-1}$) and a sinusoid, with a period of 7.9 yr and a semi-amplitude of 6.1 s. They suggested that the sinusoidal variation could be produced by an LTT effect due to a circumbinary planet in this system with a minimum mass of $2.3 M_{\text{Jup}}$ and the parabolic change may be a part of an additional period modulation due to the possible presence of a fourth object.

For ephemeris computations of NY Vir, our measurements were added to the compilation used by Kilkenny (2011) and the eclipse timings observed by Çamurdan et al. (2012) and Qian et al. (2012). First of all, we represented the minimum epochs by a parabolic least-squares fit. However, the quadratic ephemeris is not sufficiently detailed to fit all observed timings and the O–C residuals from it seem to oscillate with a very small semi-amplitude (<0.0001 d).

Table 3. New times of minimum light for NY Vir.

| BJD | Error | MIN | Note |
|----------------|------------|-----|------------------------|
| 2453509.512963 | ±0.000 001 | I | Vučković et al. (2007) |
| 2453509.563606 | ±0.000 001 | II | Vučković et al. (2007) |
| 2453509.613966 | ±0.000 003 | I | Vučković et al. (2007) |
| 2453509.664669 | ±0.000 003 | II | Vučković et al. (2007) |
| 2455589.88599 | ±0.000 05 | II | LOAO |
| 2455589.93642 | ±0.000 03 | I | LOAO |
| 2455589.98693 | ±0.000 04 | II | LOAO |
| 2455590.03749 | ±0.000 04 | I | LOAO |
| 2455590.094656 | ±0.000 05 | I | LOAO |
| 2455590.09701 | ±0.000 17 | II | LOAO |
| 2455599.88685 | ±0.000 11 | II | LOAO |
| 2455599.98762 | ±0.000 08 | II | LOAO |
| 2456000.03803 | ±0.000 07 | I | LOAO |
| 2456000.089677 | ±0.000 14 | II | LOAO |
| 2456010.04821 | ±0.000 05 | I | LOAO |
| 2456040.02814 | ±0.000 07 | II | LOAO |
| 2455598.94764 | ±0.000 02 | I | LOAO |
| 2455598.99821 | ±0.000 08 | II | LOAO |
| 2455599.04873 | ±0.000 02 | I | LOAO |
| 2455599.95780 | ±0.000 01 | I | LOAO |
| 2455960.00786 | ±0.000 13 | II | LOAO |
| 2456346.89952 | ±0.000 06 | II | LOAO |
| 2456346.95002 | ±0.000 04 | I | LOAO |
| 2456358.92060 | ±0.000 18 | II | LOAO |
| 2456358.97090 | ±0.000 03 | I | LOAO |
| 2456359.02188 | ±0.000 08 | II | LOAO |
| 2456376.85068 | ±0.000 03 | I | LOAO |
| 2456376.90136 | ±0.000 19 | II | LOAO |
| 2456376.95174 | ±0.000 04 | I | LOAO |
| 2456377.00181 | ±0.000 08 | II | LOAO |
| 2456457.66350 | ±0.000 02 | I | LOAO |
| 2456457.71401 | ±0.000 10 | II | LOAO |
| 2456457.76445 | ±0.000 03 | I | LOAO |
| 2456458.67367 | ±0.000 03 | I | LOAO |
| 2456458.72452 | ±0.000 08 | II | LOAO |
| 2456458.77466 | ±0.000 03 | I | LOAO |
| 2456724.90146 | ±0.000 15 | II | LOAO |
| 2456724.95176 | ±0.000 03 | I | LOAO |
| 2456725.00204 | ±0.000 16 | II | LOAO |
| 2456801.67332 | ±0.000 09 | II | LOAO |
| 2456801.72384 | ±0.000 03 | I | LOAO |
| 2456801.77407 | ±0.000 12 | II | LOAO |
| 2456801.82488 | ±0.000 03 | I | LOAO |

This implies that the period change of the eclipsing pair could be explained by a combination of at least two causes, a long-term period decrease and a short-term oscillation. In order to examine a circumbinary companion in the system as the possible cause of the periodic variation, it is better to use LTT rather than the pure sine curve used by Qian et al. (2012). Such an ephemeris may be represented as

$$C_1 = T_0 + PE + AE^2 + \tau_3, \quad (1)$$

where τ_3 symbolizes the LTT due to a third body (Irwin 1952). Because the secondary eclipses are much shallower and their timings less determinate than the primary ones, no secondary eclipses were used in our timing analyses. In addition, we excluded primary eclipse times with quoted errors larger than 0.0001 d. For the timings without errors published by Kilkenny et al. 2000, their standard deviation of ±0.000 03 d was calculated to provide a mean error. Weights for all timings were then scaled as the inverse squares of their errors.

The Levenberg–Marquart (LM) algorithm (Press et al. 1992) was applied to evaluate the eight parameters of the ephemeris (Irwin 1959). Initial parameter values were obtained from Qian et al. (2012) and a periodogram analysis for the timing data and orbital eccentricities between 0 and 1 were examined. The results are summarized in the second column of Table 4, together with physical parameters derived by applying the absolute parameters ($M_1 = 0.466 M_{\odot}$, $M_2 = 0.122 M_{\odot}$, $R_1 = 0.15 R_{\odot}$, $R_2 = 0.16 R_{\odot}$, $L_1 = 19.3 L_{\odot}$, and $L_2 = 0.003 L_{\odot}$) from Model II in table 3 of Vučković et al. (2007). The LM technique produces the formal errors computed from the best-fitting covariance matrix. Thus, we determined the parameter errors from Monte Carlo bootstrap-resampling experiments (Press et al. 1992, Hinse et al. 2014b). For this, we generated 50 000 bootstrap-resampling data sets and used the best-fitting model as our initial guess for each data set. The parenthesized numbers in Table 4 are the 1σ values associated with the last digits of the evaluations. We use the best-fitting values as the average to compute the standard deviation from the 50 000 element bootstrap array. The orbital period of the third body in an eccentric orbit of $e_3 = 0.46$ is somewhat longer than that determined by Qian et al. (2012). In the top panel of Fig. 2, the solid and parabolic curves represent the full contribution and the quadratic term of the equation, respectively. The middle panel refers to the LTT orbit with a cycle length of 8.42 yr and the bottom panel displays the residuals from the full ephemeris. The quadratic plus LTT ephemeris gives a satisfactory fit to the mean trend of the timing residuals and results in a smaller $\chi^2_{\text{red}} = 1.31$ than the parabolic ephemeris ($\chi^2_{\text{red}} = 2.08$), although even C_1 does not fit well with the 2014 timings.

The downward parabolic curve in Fig. 2 cannot be explained by a mass transfer between the binary components, because the eclipsing pair is a very detached system and both stars are close to spheres. Hence, the long-term period decrease at a rate of $-3.36 \times 10^{-9} \text{ d yr}^{-1}$ can be interpreted as AML corresponding to $dJ/dt = -1.38 \times 10^{35} \text{ cgs units}$. Possible mechanisms for AML are gravitational radiation (Paczynski 1967) and/or magnetic braking in the cool secondary (Rappaport, Verbunt & Joss 1983). We computed the AML rate for each mechanism in a procedure identical to that for HW Vir (Lee et al. 2009a). The theoretical rate for gravitational radiation is -1.01×10^{33} , which is about two orders of magnitude smaller than the observed value, while the AML rate for the latter is -2.07×10^{35} for $\gamma = 2$, all in cgs units. Added to our previous evaluation for HW Vir, this result makes it likely that the secular period decreases of sdB+M eclipsing binaries are mainly produced by AML due to magnetic stellar wind braking. However, because the secondary component should be a fully convective star, it may be that the magnetic braking may not be a dominant contributor to the observed period decrease of NY Vir.

Another mechanism may be needed to explain the secular change. It is alternatively possible that the quadratic term can be just the observed part of a second LTT effect due to the existence of a more distant circumbinary object. Accordingly, the times of minimum light were fitted to a two-LTT ephemeris, as follows

$$C_2 = T_0 + PE + \tau_3 + \tau_4. \quad (2)$$

The LM method was used again in order to simultaneously evaluate the LTT parameters of the third and newly assumed fourth bodies. In this process, we have explored a large number of initial guesses for the LM method. Final results are given in the third and fourth columns of Table 4. We found that the parameter errors determined from the LM algorithm are too optimistic and underestimated and, thus, determined the parameter errors from 50 000 bootstrap-resampling simulations in a manner similar to that for

Table 4. Parameters for the LTT orbits of NY Vir.

| Parameter | Quadratic plus LTT | | Two-LTT | Unit |
|-----------------------|-----------------------------|---------------------------|---------------------------|---------------------|
| | τ_3 | τ_3 | τ_4 | |
| T_0 | 2453174.4429776(62) | | 2453174.442699(91) | BJD |
| P | 0.101 015 968 16(37) | | 0.101 015 9668(43) | d |
| $a_{12}\sin i_{3,4}$ | 0.0160(13) | 0.0153(22) | 0.055(16) | au |
| e | 0.46(18) | | 0.44(17) | 0.00(20) |
| ω | 314.0(3.0) | 346(15) | 333(15) | deg |
| n | 0.1171(33) | 0.1205(27) | 0.0365(50) | deg d ⁻¹ |
| T | 2453167(40) | 2453472(141) | 2450031(497) | BJD |
| $P_{3,4}$ | 8.42(23) | 8.18(18) | 27.0(3.7) | yr |
| K | 7.57(60) | 6.9(1.0) | 27.3(8.2) | s |
| $f(M_{3,4})$ | $5.79(49) \times 10^{-8}$ | $5.34(76) \times 10^{-8}$ | $2.25(74) \times 10^{-7}$ | M_\odot |
| $M_{3,4}\sin i_{3,4}$ | 2.85(11) | 2.78(19) | 4.49(72) | M_{Jup} |
| $a_{3,4}\sin i_{3,4}$ | 3.457(69) | 3.39(12) | 7.54(64) | au |
| A | $-4.65(12) \times 10^{-13}$ | | | d |
| dP/dr | $-3.36(10) \times 10^{-9}$ | | | d yr ⁻¹ |
| rms scatter | 3.39 | | 2.83 | s |
| χ^2_{red} | 1.31 | | 1.09 | |

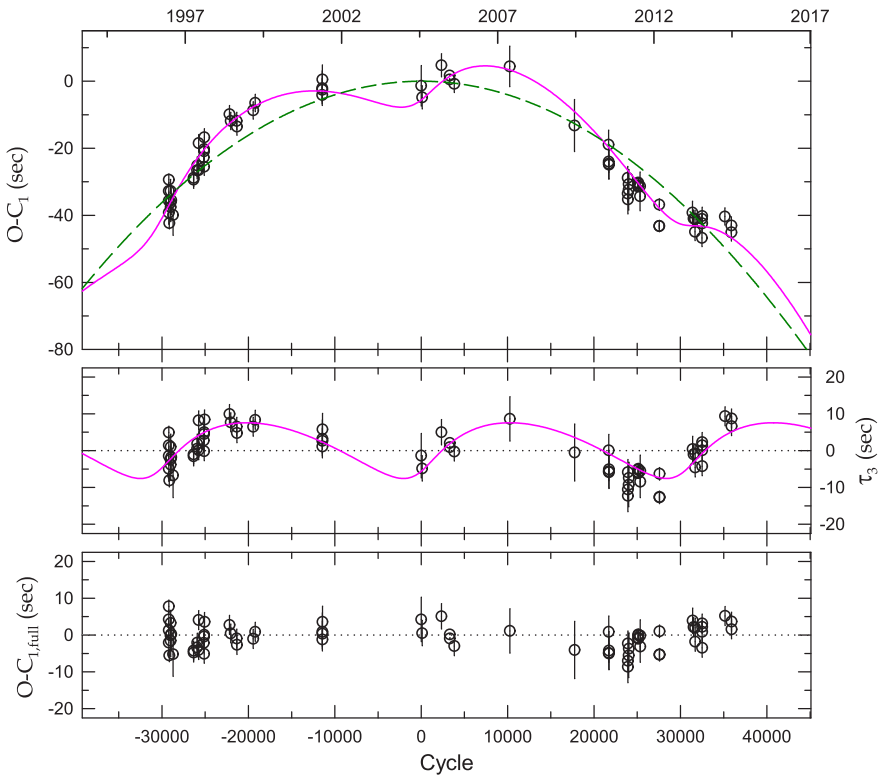


Figure 2. O – C₁ diagram of NY Vir constructed with the linear terms of the quadratic plus LTT ephemeris. In the top panel, the solid curve and the dashed parabola represent the full contribution and the quadratic term of the equation, respectively. The middle panel displays the LTT orbit with a cycle length of 8.42 yr and the bottom panel shows the residuals from the full ephemeris.

the quadratic plus LTT ephemeris. The short-term periods for the two ephemerides agree with each other within the limits of their errors. The O–C₂ diagram with respect to the two-LTT ephemeris is drawn at the uppermost panel of Fig. 3 with the solid curve due to the full effect of equation (2). The second and third panels display the τ_3 and τ_4 orbits, respectively, and the bottom panel shows the residuals from the complete ephemeris. The observed scatters seen in the O–C_{2,full} residuals may be affected by the rapid multimode pulsations of the sdB primary star. The short-term orbit of τ_3 has a relatively high determinacy because the observations have

already covered about two cycles, while the long-term orbit of τ_4 is currently preliminary because only about 67 per cent of the 27-yr period has been covered.

4 ORBITAL STABILITY OF TWO-PLANET SYSTEM

At this stage the most likely interpretation of the period change is that it is due to two planets, and this raises the question of their orbital time evolution. In recent times, the orbital stability of

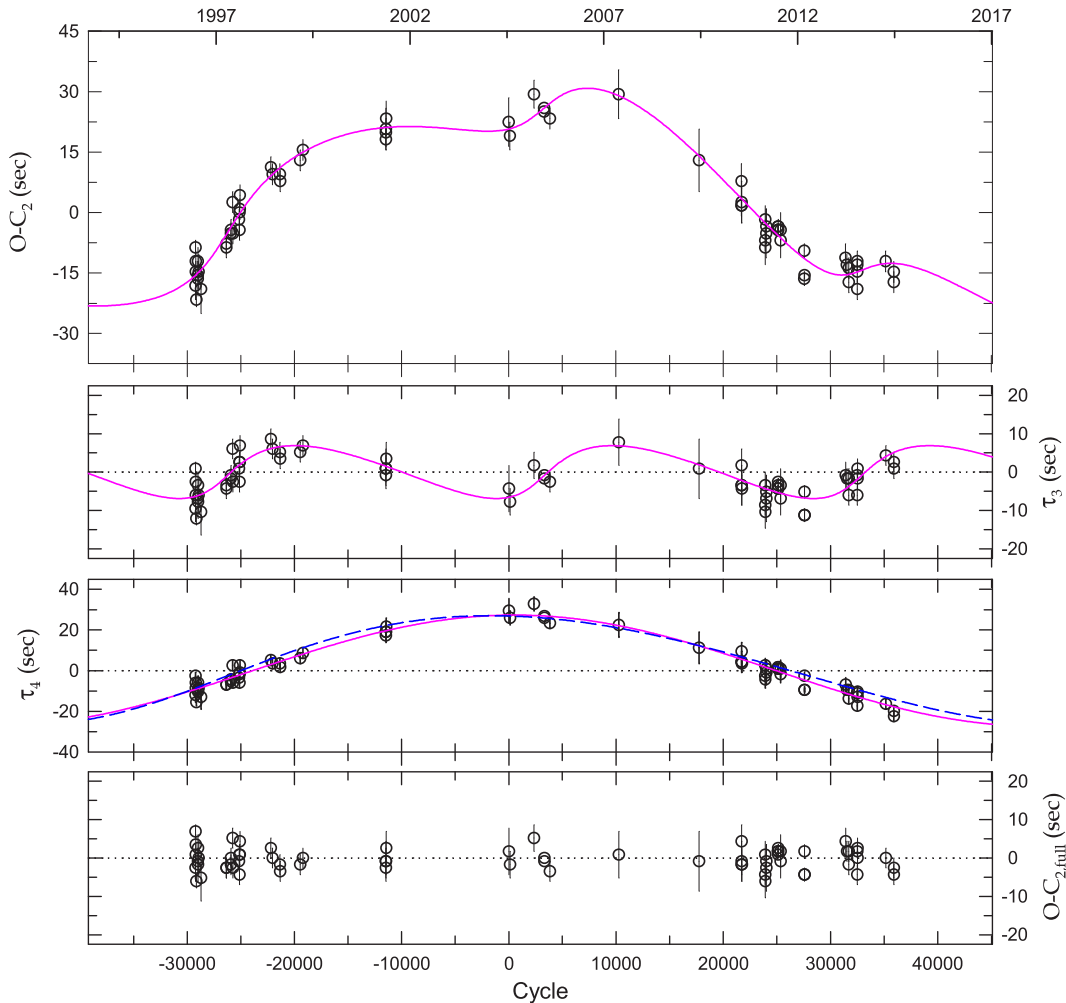


Figure 3. $O - C_2$ diagram of NY Vir with respect to the two-LTT ephemeris. In the uppermost panel, the continuous curve represents the full effect of equation (2). The second and third panels display the short-term (τ_3) and long-term (τ_4) LTT orbits, respectively. The bottom panel shows the residuals from the complete ephemeris. The dashed curve in the third panel is the LTT model corresponding to the black dot ($e_4 = 0.17$) of Fig. 5(b).

proposed multibody circumbinary systems detected from timing measurements has been studied by Horner et al. (2011), Hinse et al. (2012) and Hinse et al. (2014a, and references therein). An orbital stability check can be used as an independent test of the feasibility of our two-companion model. We have therefore carried out a stability study for the best-fitting orbit parameters of NY Vir in Table 4, under the assumption that the combined mass ($0.588 M_\odot$) of the eclipsing pair can be considered as a central object and that the binary perturbations are negligible. Using the variable time-step RADAU algorithm implemented in the MERCURY integration package (Chambers 1999), we computed several batches of single-orbit integrations considering various initial conditions. The total integration time span was 10^6 yr. In detail, we considered orbits within the errors obtained from the bootstrap-resampling technique. In addition giving the uncertainty in the time of pericentre passage, we started the two planets from various initial mean longitudes. Furthermore, since their masses are minimum values we also considered various inclinations and scaled the masses of the companions accordingly.

In most cases we found the system to exhibit large-scale orbital instabilities. Instability occurs either due to ejection from the system or any pair of body collide with each other. In the top panel of Fig. 4, we show the time evolution of the semimajor axes and eccentricities of the two companions for the best-fitting model (Table 4)

demonstrating an ejection of the outer companion after $\simeq 850\,000$ yr. The result is in contrast with our expectation that the system should be stable following bounded orbits. However, while still considering best-fitting parameters, we then explored the system's orbital time evolution for the upper limit of the outer companion's eccentricity and encountered stable/quasi-periodic orbits with no sign of chaotic dynamics. In an attempt to study the dynamics of the two-planet system in some more detail, we have numerically explored the phase space of the outer companion in a neighbourhood of its best-fitting orbit including the 1σ parameter errors obtained from the bootstrap-resampling technique. As an example we present the results of considering three (minimum, nominal best-fitting and maximum) initial eccentricities within the orbital error range of the inner companion.

We calculated the lifetime (Horner et al. 2011) and the MEGNO¹ factor ((Y)) (Cincotta & Simó 2000; Goździewski, Bois & Maciejewski 2002) over a large set of orbits in the semimajor axis-eccentricity space of the outer companion. For this task we used the MECHANIC/MPI orbit integration package (Słonina, Goździewski & Migaszewski 2015). The results are shown in Fig. 5. In each panel

¹ Mean Exponential Growth Factor of Nearby Orbits.

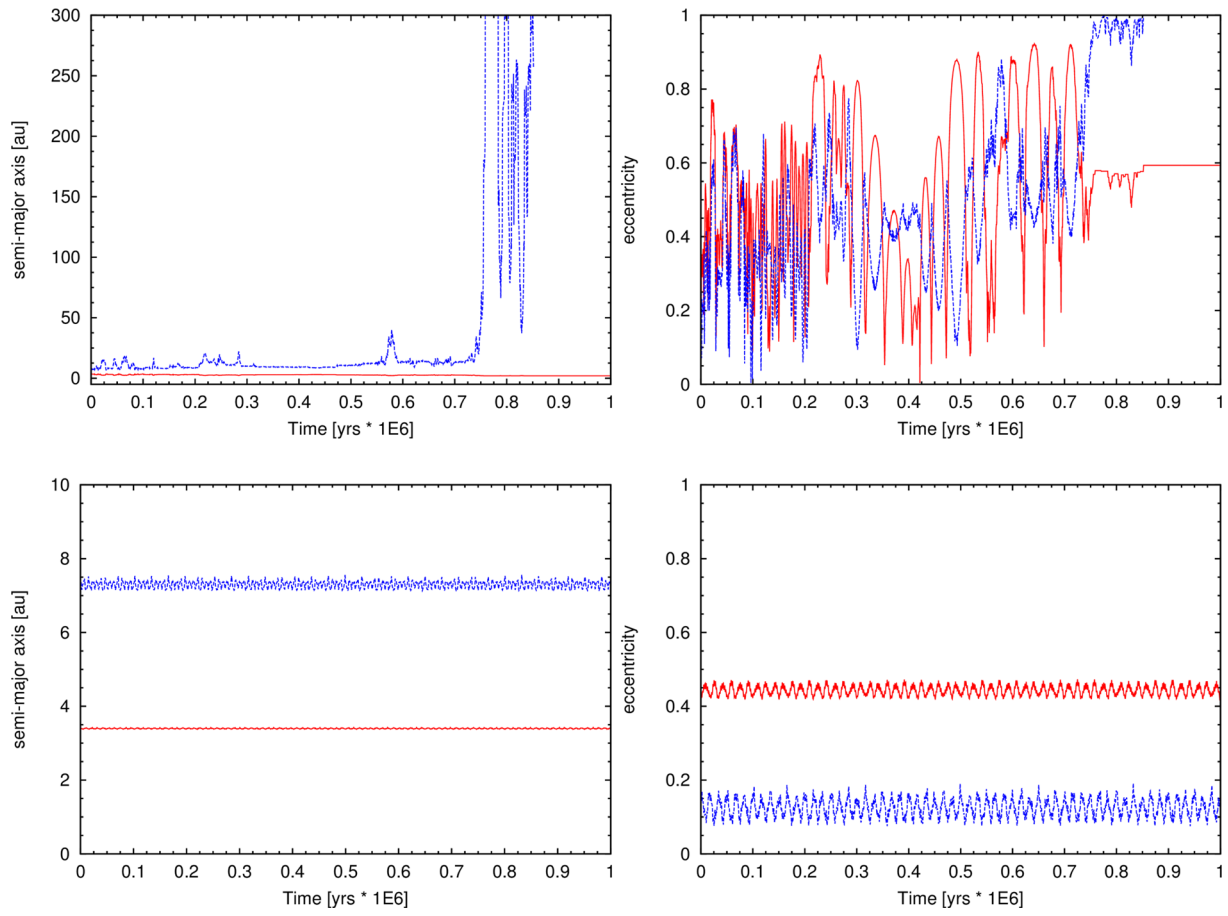


Figure 4. Orbital time evolution of the inner (red) and outer (blue) companions over 10^6 yr using the RADAU algorithm. Top panel: initial conditions are taken to be best-fitting model parameters as shown in Table 4. The temporal evolution clearly shows a strong gravitational interaction between the two proposed companions, resulting in the ejection of the outer companion after 850 000 yr due to a mutual close encounter. Bottom panel: hypothetical case of placing the outer companion at the black dot shown in Fig. 5(b) (middle panel). All other parameters are taken to be best-fitting values of the two-LTT model. The two companions are now perturbing each other on smaller magnitudes and the system follows long-lived orbits over at least a one-million year time-scale.

the parameter error box in the semimajor axis-eccentricity space of the outer companion is shown by a thick vertical and horizontal line centred on the nominal best-fitting values. The left-side panels shows the degree of chaotic time evolution of the system for various initial conditions of the outer companion. Regions with colours $\langle Y \rangle \sim 2$ follow quasi-periodic orbits. All other orbits follow chaotic orbits. The right-side panels of Fig. 5 shows the lifetime of the system (determined in the event of ejection or collision). As shown earlier the best-fitting orbit of the outer companion is embedded in a region of high chaoticity and relatively short system lifetime.

As an example of a bounded orbit we have followed the dynamical time evolution of the initial condition shown by a black dot in Fig. 5 located at a semimajor axis corresponding to the best-fitting value of the outer companion's semimajor axis. The eccentricity of the outer companion was chosen to be 0.17 well within the uncertainty range of 0.20 (and 17 per cent larger than the best-fitting value). The time evolution of the orbit is shown in the bottom panel of Fig. 4 now demonstrating that the system is stable with bounded quasi-periodic orbits over 10^6 yr with no sign of stochastic/random walk in the orbital elements during that time period. The corresponding LTT model is plotted as a dashed curve in the third panel of Fig. 3. However, we would like to point out that the outer companion's orbit is not well characterized with the current data set.

5 SUMMARY AND DISCUSSION

The successful fit to the eclipse times reveals that the orbital period of NY Vir has varied due to a combination of two periodic oscillations with cycle lengths of $P_3 = 8.2$ yr and $P_4 = 27.0$ yr and semi-amplitudes of $K_3 = 6.9$ s and $K_4 = 27.3$ d, respectively. The sinusoidal variations, shown in the second and third panels of Fig. 3, can reasonably be interpreted as a pair of LTT effects driven by two substellar objects with minimum masses of $M_3 \sin i_3 = 2.8 M_{\text{Jup}}$ and $M_4 \sin i_3 = 4.5 M_{\text{Jup}}$. Assuming the circumbinary objects to be in the orbital plane ($i = 81^\circ$) of the eclipsing pair, the masses of the third and fourth components would match to giant planets. The period ratio of P_3/P_4 implies that the two companions are located close to the 3:10 mean motion resonance. To the best of our knowledge, the result would be the fifth case when two circumbinary companions would be in or close to any kind of resonance (cf. Lee et al. 2012a). This suggests that a long-term gravitational interaction between the two planets would result in capture into the 3:10 resonant configuration.

Although all historical timings agree quite well with the calculated LTT effects as seen in Fig. 3, we cannot a priori exclude the possibility that the period modulations in the eclipse timing diagram are due to magnetic activity cycles in the M-type secondary star. Therefore, we studied this alternate interpretation. With the

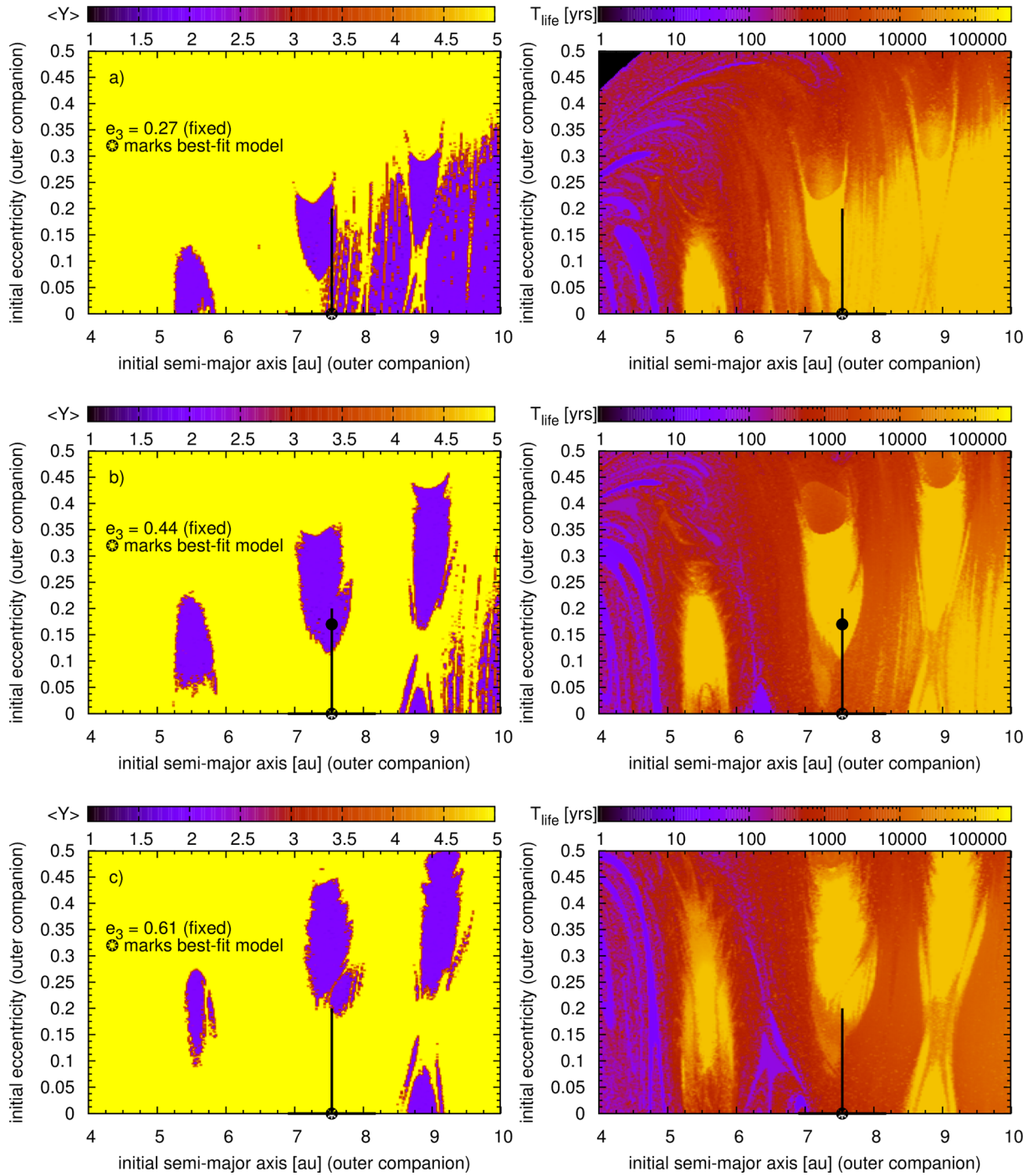


Figure 5. Dynamical maps and orbital parameter survey of the outer companion using the MECHANIC orbit integration package. A given integration is terminated if the distance of any object reached 100 au or in the event of an ejection/collision or for $\langle Y \rangle > 12$. The best-fitting semimajor axis (7.54 au) is shown with a vertical line. The parameter uncertainty in the semi-major axis and eccentricity of the outer companion is shown. The black dot indicates the location of a hypothetical initial condition rendering the overall system to become stable and long-lived. Left-hand panels: MEGNO map of initial conditions in the neighbourhood of the outer companion for three different eccentricities (initially fixed to its minimum, nominal best-fitting and maximum value) of the inner companion. Regions with quasi-periodic (bounded) orbits result in $\langle Y \rangle \sim 2$ while strongly chaotic orbits have $\langle Y \rangle \gg 5$. Right-hand panels: corresponding lifetime map considering the same parameter range. A clear correlation between quasi-periodic and long-lived orbits is evident.

modulation period ($P_{3,4}$) and amplitude (K) for the sinusoidal variations, model parameters were obtained from the formulae given by Applegate (1992). According to this theory, the secondary star with only $0.003 L_\odot$ should exhibit the predicted luminosity variations of $\Delta L_{\text{rms},3} \gtrsim 0.0012 L_\odot$ and $\Delta L_{\text{rms},4} \gtrsim 0.0005 L_\odot$ for the short-term

and long-term period variations, respectively, which is about 4.0 and 1.7 times larger than the $\Delta L_{\text{rms}}/L_2 \sim 0.1$ level he proposed. Moreover, the timing analyses for HW Vir (Lee et al. 2009a) and HS 0705+6700 (Qian et al. 2009) indicated that it is difficult for the model to produce the perfectly smooth periodic variations of

the sdB+M eclipsing pairs. These mean that Applegate's mechanism cannot contribute significantly to the observed period change of NY Vir. On the other hand, a single periodic variation could be attributed to apsidal motion in an elliptical orbit (cf. Parsons et al. 2014). However, previous studies for NY Vir suggest that the binary orbit is circular which in turn excludes timing variations from apsidal precession.

Because all other mechanisms (Applegate effect, apsidal motion, and AML) of the period change can be ruled out, the most likely explanation of the variation is a pair of LTT effects driven by the presence of circumbinary companions. However, we found the two best-fitting orbits to result in the ejection of the outer companion after some 800 000 yr. This time span is considerably longer than the lifetimes of previously studied circumbinary multibody systems (Horner et al. 2012a,b, 2013; Wittenmyer et al. 2012; Wittenmyer, Horner & Marshall 2013). With the limited span of timing measurements the outer companion orbit is still lacking a firm characterization. We have therefore explored the neighbourhood of the best-fitting orbit and found several regions in phase space for which the system exhibits bounded orbits over 10^6 yr. Future timing measurements will further characterize the outer companion and we conjecture that the best-fitting eccentricity for the outer companion will increase to produce long-lived stable orbits. On the other hand, the root-mean-square (rms) scatter of timing measurements around our two-LTT model is 2.8 s. Compared with the semi-amplitude of the inner LTT orbit of 7 s, the detection of the inner companion is only marginal with a formal detection significance of 2.5σ . This fact should motivate obtaining precise timing measurements better than ~ 3 s to identify and understand the proposed planetary system.

Up to now, the possible presences of circumbinary companions have been reported in 5 of 13 known HW Vir-type eclipsing systems including NY Vir: HW Vir (Lee et al. 2009a; Beuermann et al. 2012), HS 0705+6700 (Qian et al. 2009, 2013), HS 2231+2441 (Qian et al. 2010), and NSVS 14256825² (Almeida, Jablonski & Rodrigues 2013). All the companions are likely either massive planets or BDs based on their masses. How and when, then, did the circumbinary objects in the eclipsing system form? Typically, BDs are built up by fragmentation of a protostellar cloud, while planets originate from a protoplanetary disc left over from the protostellar disc of their newly formed host star (Udry & Santos 2007). Perets (2010, 2011) suggested that a circumbinary planet orbiting the evolved binaries formed from protoplanetary disc material (first generation), from the secondary generation disc formed in the ejected envelope during post-MS evolution (second generation), or by the scattering of an S-type circumstellar planet into a circumbinary orbit. The second generation planets form in much older systems than the first generation ones and have a different source of material. If the circumbinary companions in the sdB+M eclipsing systems are formed in the first generation disc, their masses might be increased by accreting a large amount of the material replenished during the post-MS evolution. In consequence, more massive planets could become BD companions and be found in the BD dessert regime. At present, it is difficult to differentiate between the two types of substellar populations and additional information on such circumbinary objects is needed. The discovery and study of the circumbinary substellar objects around old evolved binary systems could shed new light on our understanding of both planet formation

²A recent detailed study by Hinse et al. (2014a) indicates that the planets proposed in NSVS 14256825 are not feasible and the eclipse timing data are insufficient to reliably constrain the LTT model.

and binary evolution. In the case of the eclipsing system NY Vir, because the primary component is a pulsating sdB star like V391 Peg (Silvotti et al. 2007), the pulsations can be used as an independent tool to confirm the circumbinary planets discovered by the eclipse timings.

ACKNOWLEDGEMENTS

The authors wish to thank Dr Maja Vučković for sending us their VLT/ULTRACAM photometric data. The authors also thank the staffs of LOAO for assistance with our observations. We appreciate the careful reading and valuable comments of the anonymous referee. This research has made use of the Simbad data base maintained at CDS, Strasbourg, France, and was supported by the KASI (Korea Astronomy and Space Science Institute) grant 2014-1-400-06. Numerical simulations were carried out on the KMTNet computing cluster at KASI and the SFI/HEA Irish Centre for High-End Computing (ICHEC).

REFERENCES

- Almeida L. A., Jablonski F., Rodrigues C. V., 2013, ApJ, 766, 11
- Applegate J. H., 1992, ApJ, 385, 621
- Beuermann K., Dreizler S., Hessman F. V., Deller J., 2012, A&A, 543, 138
- Çamurdan C. M., Çamurdan D. Z., İbanoğlu C., 2012, New Astron., 17, 325
- Chambers J., 1999, MNRAS, 304, 793
- Cincotta P., Simó C., 2000, ApJS, 147, 205
- Doyle L. R., Deeg H.-J., 2004, in Norris R., Stootman F., eds, Proc. IAU Symp. 213, Bioastronomy 2002: Life Among the Stars. Astron. Soc. Pac., San Francisco, p. 80
- Eastman J., Siverd R., Gaudi B. S., 2010, PASP, 122, 935
- Goździewski K., Bois E., Maciejewski A. J., 2002, MNRAS, 332, 839
- Hinse T. C., Goździewski K., Lee J. W., Haghighipour N., Lee C. U., 2012, AJ, 144, 34
- Hinse T. C., Lee J. W., Goździewski K., Horner J., Wittenmyer R. A., 2014a, MNRAS, 438, 307
- Hinse T. C., Horner J., Lee J. W., Wittenmyer R. A., Lee C.-U., Park J.-H., Marshall J., 2014b, A&A, 565, 104
- Holman M. J., 2005, Science, 307, 1288
- Horner J., Marshall J. P., Wittenmyer R. A., Tinney C. G., 2011, MNRAS, 416, L11
- Horner J., Wittenmyer R. A., Hinse T. C., Tinney C. G., 2012a, MNRAS, 425, 749
- Horner J., Hinse T. C., Wittenmyer R. A., Marshall J. P., Tinney C. G., 2012b, MNRAS, 427, 2812
- Horner J., Wittenmyer R. A., Hinse T. C., Marshall J. P., Mustill A. J., Tinney C. G., 2013, MNRAS, 435, 2033
- Hu H., Nelemans G., Østensen R. H., Aerts C., Vučković M., Groot P. J., 2007, A&A, 473, 569
- Irwin J. B., 1952, ApJ, 116, 211
- Irwin J. B., 1959, AJ, 64, 149
- Kilkenny D., 2011, MNRAS, 412, 489
- Kilkenny D., O'Donoghue D., Koen C., Lynas-Gray A. E., van Wyk F., 1998, MNRAS, 296, 329
- Kilkenny D., Keuris S., Marang F., Roberts G., van Wyk F., Ogloza W., 2000, The Observatory, 120, 48
- Kilkenny D. et al., 2003, MNRAS, 345, 834
- Kwee K. K., van Woerden H., 1956, Bull. Astron. Inst. Neth., 12, 327
- Lee J. W., Kim S.-L., Kim C.-H., Koch R. H., Lee C.-U., Kim H.-I., Park J.-H., 2009a, AJ, 137, 3181
- Lee J. W., Youn J.-H., Lee C.-U., Kim S.-L., Koch R. H., 2009b, AJ, 138, 478
- Lee J. W., Youn J.-H., Kim S.-L., Lee C.-U., Koo J.-R., 2011, PASJ, 63, 301
- Lee J. W., Lee C.-U., Kim S.-L., Kim H.-I., Park J.-H., 2012a, AJ, 143, 34
- Lee J. W., Youn J.-H., Kim S.-L., Lee C.-U., Hinse T. C., 2012b, AJ, 143, 95

- Paczynski B., 1967, *Acta Astron.*, 17, 287
 Parsons S. G. et al., 2014, *MNRAS*, 438, L91
 Perets H. B., 2010, preprint ([arXiv:1001.0581](https://arxiv.org/abs/1001.0581))
 Perets H. B., 2011, in Schuh S., Drechsel H., Heber U., eds, AIP Conf. Proc. Vol. 1331, Planetary Systems Beyond the Main Sequence. Am. Inst. Phys., New York, p. 56
 Press W. H., Teukolsky S. A., Vetterling W. T., Flannery B. P., 1992, Numerical Recipes. Cambridge Univ. Press, Cambridge, p. 773
 Pribulla T. et al., 2012, *Astron. Nachr.*, 333, 754
 Qian S.-B. et al., 2009, *ApJ*, 695, L163
 Qian S.-B. et al., 2010, *Ap&SS*, 329, 113
 Qian S.-B., Zhu L.-Y., Dai Z.-B., Fernández Lajús E., Xiang F.-Y., He J.-J., 2012, *ApJ*, 745, L23
 Qian S.-B. et al., 2013, *MNRAS*, 436, 1408
 Rappaport S., Verbunt F., Joss P. C., 1983, *ApJ*, 275, 713
 Silvotti R. et al., 2007, *Nature*, 449, 189
 Slonina M., Goździewski K., Migaszewski C., 2015, *New Astron.*, 34, 98
 Udry S., Santos N. C., 2007, *ARA&A*, 397
 Vučković M., Aerts C., Østensen R. H., Nelemans G., Hu H., Jeffery C. S., Dhillon V. S., Marsh T. R., 2007, *A&A*, 471, 605
 Vučković M., Østensen R., Aerts C., Telting J. H., Heber U., Oreiro R., 2009, *A&A*, 505, 239

- Wittenmyer R. A., Horner J., Marshall J. P., Butters O. W., Tinney C. G., 2012, *MNRAS*, 419, 3258
 Wittenmyer R. A., Horner J., Marshall J. P., 2013, *MNRAS*, 431, 2150

SUPPORTING INFORMATION

Additional Supporting Information may be found in the online version of this article:

Table 2. *I*-band photometry of NY Vir(<http://mnras.oxfordjournals.org/lookup/suppl/doi:10.1093/mnras/stu1937/-DC1>).

Please note: Oxford University Press are not responsible for the content or functionality of any supporting materials supplied by the authors. Any queries (other than missing material) should be directed to the corresponding author for the paper.

This paper has been typeset from a \TeX / \LaTeX file prepared by the author.